Accepted Manuscript

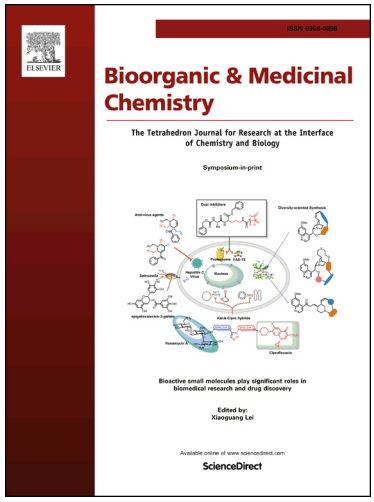

Synthesis, biological evaluation and molecular modeling of imidazo[1,2-*a*]pyridine derivatives as potent antitubulin agents

Jin Liu, Daiying Zuo, Tongfei Jing, Ming Guo, Lingyun Xing, Wenyu Zhang, Jianwen Zhao, Jiwei Shen, Ping Gong, Dajun Zhang, Xin Zhai

PII: S0968-0896(17)30821-0
DOI: http://dx.doi.org/10.1016/j.bmc.2017.05.057
Reference: BMC 13776

To appear in: *Bioorganic & Medicinal Chemistry*

Received Date: 18 April 2017
Revised Date: 15 May 2017
Accepted Date: 27 May 2017

Please cite this article as: Liu, J., Zuo, D., Jing, T., Guo, M., Xing, L., Zhang, W., Zhao, J., Shen, J., Gong, P., Zhang, D., Zhai, X., Synthesis, biological evaluation and molecular modeling of imidazo[1,2-*a*]pyridine derivatives as potent antitubulin agents, *Bioorganic & Medicinal Chemistry* (2017), doi: http://dx.doi.org/10.1016/j.bmc.2017.05.057

Synthesis, biological evaluation and molecular modeling of imidazo[1,2-*a*]pyridine derivatives as potent antitubulin agents

Jin Liu[1,#], Daiying Zuo[1,#], Tongfei Jing[1], Ming Guo[1], Lingyun Xing[1], Wenyu Zhang[1], Jianwen Zhao[2], Jiwei Shen[1], Ping Gong[1], Dajun Zhang[2,*], Xin Zhai[1,*]

[1]*Key Laboratory of Structure-Based Drug Design and Discovery,Ministry of Education, Shenyang Pharmaceutical University, Shenyang 110016, PR China;*[2]*key lab. of behavioral and cognitive neuroscience of Liaoning province, Shenyang Medical College, Shenyang 110034, PR China.*

Abstract

Two series of novel 5,7-diarylimidazo[1,2-*a*]pyridine-8-carbonitrile derivatives (**3a-3q** and **7a-7n**) were designed by modification of CA-4 pharmacophore to develop colchicine targeted antitubulin agents. All compounds were efficiently synthesized and evaluated for their cytotoxicity against five selected cancer cell lines (HT-29, H460, A549, MKN-45 and SMMC-7721) which got an insight in structure and activity relationships (SARs). Several molecules (**7e, 7f, 7h-7j** and **7m**) were disclosed to exhibit promising antiproliferative activity with IC_{50} values in double-digit nanomolar degree. Optimization toward these compounds led to the discovery of a promising lead **7e**, which showed noteworthy potency with IC_{50} value ranging from 0.01 to 3.2 μM superior to CA-4 and Crolibulin. Importantly, immunofluorescence staining and colchcine competitive binding assay revealed that microtubule dynamics was disrupted by **7e** by binding at the colchicine site of tubulin. Moreover, molecular docking studies suggested the binding of this mimic at colchcine-binding site is similar to Crolibulin, as was in conformity with the observed SARs for these compounds.

Keywords: Imidazo[1,2-*a*]pyridines; Tubulin; Synthesis; Cytotoxicity; Molecular modeling

1. Introduction

Microtubules are a key cytoskeletal structure which exert their effects by disrupting microtubule dynamics and inhibiting the noncovalent polymerization of tubulin into microtubules, resulting in disruption of cell progression, signal transduction and, subsequently, induction of cell death [1-2]. The essential role of microtubules in mitotic spindle formation makes them one of the most attractive targets for development of antitumor molecules [3-5]. There are four main binding sites on tubulin which include *colchicine* site, *vinca* domain, *taxane* site and *laulimalide* domain [6-8] and some of the well-known natural occurring tubulin binding ligands that inhibit microtubule dynamics by binding to the distinct colchicine domains are colchicine [9], combretastatin A-4(CA-4) [10], Crolibulin [11], and diverse hit-like synthetic antitubulin ligands [12-14] (Fig. 1).

CA-4, a natural antitubulin agent isolated from South Africa tree *Combretumcaffrum*, was reported to inhibit microtubules dynamics strongly by binding to the colchicine site and showed excellent cytotoxicity [15]. However, the poor solubility and acquired significant toxicity toward

*Corresponding author. E-mail address: zhangdajun2008@126.com (D.J. Zhang); zhaixin_syphu@126.com (X. Zhai).

[#] Authors contributed equally to this work.

normal cells impinged its clinical development and thus, stimulated a surge of research endeavors in discovery of more effective CA-4 structurally analogs [16]. CA-4 is usually divided into three pharmacological substructures, two hydrophobic aryl rings (A and B) and a *cis*-olefin linkage. Since 3,4,5-trimethoxyaryl (A-ring) and *cis*-olefin linking bridge are generally believed to be essential for biological activity, previous structural modification was mainly focused on B-ring [17]. When we explored the relevant CA-4 literature, it was found that dihalogenation with either bromine or iodine was a tolerated modification when compared to the parent compound CA-4 and had less effect than B-ring modification on potency [18]. Therefore, 2,3,4-trimethoxyphenyl, 2,4-diflourophenyl or 2-chloro-4-flourophenyl groups were introduced to A-ring in this paper to extending the SARs. Besides, it is noteworthy that several attempts have been reported to modify the *cis*-olefin to prevent its isomerization under storage and metabolism, which led to the development of diverse CA-4 derivatives with a five to six member heteroaromatic rings, for instance, indolyl and imidazolyl as *cis*-restricted CA-4 analogues (e.g. compounds **a** in Fig. 1) [12-14].

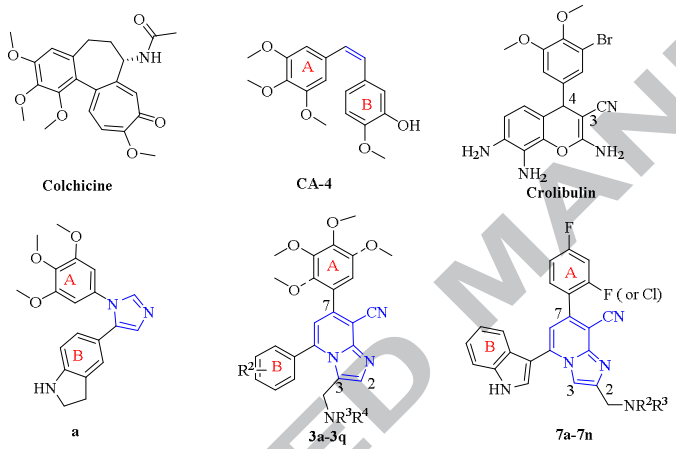

Figure 1.The colchicine-site-binding antitubulincandidates and compounds **3a-3q** and **7a-7n**.

Crolibulin, a 4-aryl-4*H*-chromene derivative in phase II clinical trials, is one of the best characterized antimitotic agents with potent vascular disrupting activity and *in vivo* efficacy [11, 19-20] (Fig. 1). Crolibulin-based SARs studies suggested that the cyano group at C-3 position is essential for its antitumor potency, and substituted phenyl are the preferred group at C-4 position of 4*H*-chromenes [11, 21].

Imidazo[1,2-*a*]pyridines (IMPs) framework was recognized as a "drug prejudice" scaffold due to its diverse biological activities and adopted in a variety of clinical drugs [22-25]. Herein, our researches have been focused on optimization of the 4-aryl-4*H*-chromenes-3-carbonitrile scaffold of Crolibulin by replacing with imidazo[1,2-*a*]pyridine-8-carbonitrile fragment.

In our effort to search for antitubulin agents targeting colchicines-binding site, we were inspired to further optimize the 7-arylimidazo[1,2-*a*]pyridine-8-carbonitrile skeleton by introducing aryl group at C-5 position as the B-ring based on bioisosterism and molecular hybridization principles. In the continuation of SARs study of restricted CA-4 derivatives, the B-ring was replaced by the pharmacologically relevant phenyl or indolyl scaffolds, and the *cis* configuration of olefin was restricted by incorporation of imidazo[1,2-*a*]pyridine-8-carbonitrile framework which is envisaged by the structural resemblance to CA-4. Moreover, substituted dimethoxyphenyl or halogenated phenyl motifs were incorporated into the C-7 position to mimic CA-4. Additionally, with the

purpose of increasing water solubility, various hydrophilic *N*-aliphatic aminomethyl groups were drawn into C-2 or C-3 positions on the IMPs skeleton. Accordingly, two series of 5,7-diarylimidazo[1,2-*a*]pyridine-8-carbonitrile derivatives (**3a-3q** and **7a-7n**) were designed and synthesized. Wherein, diverse substituents were introduced to aryl groups (A and B) and terminal aminomethyl fragments in an attempt to investigate the influence on antitumor efficacy by regulating the electronic and steric effects.

In this paper, all newly synthesized compounds were evaluated for their cytotoxic activities against a panel of human cancer cell lines *in vitro*. Also, the antitubulin potency of candidate **7e** was identified by immunofluorescence staining and colchcine competitive binding assay, and the results were further confirmed by molecular docking mode analysis.

2. Chemistry

The target compounds **3a-3q** and **7a-7n** were synthesized according to the pathways depicted in Schemes 1-2. As shown in Scheme 1, 2-amino-4,6-diarylnicotinonitrile skeleton of **1a-1c** was concisely assembled in a one-pot 4-component reaction with commercially available aromatic formaldehyde, substituted acetophenones and malononitrile in the presence of ammonium acetate in refluxing toluene [26]. Subsequently, **1a-1c** were cyclization with 40% acetaldehyde in refluxing ethanol on exposure to sodium bicarbonate afforded intermediates **2a**-**2c** in good yields [27]. Finally, **2a**-**2c** were subjected to Mannich reaction at the existence of *N*-aliphatic amines and formaldehyde in acetic acid at 30 ºC, and the resultant crude products were purified by chromatography on silica gel using CH_2Cl_2/MeOH (20:1) to generate the desired compounds **3a-3q**.

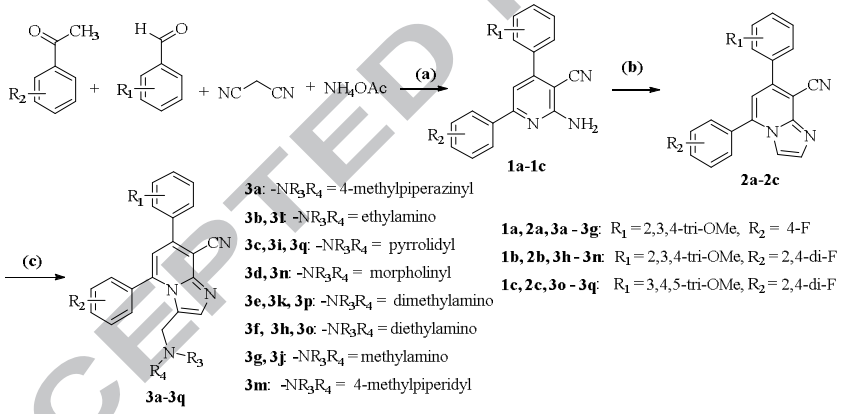

Scheme 1. Reagents and conditions: (a) toluene, reflux; (b) 40% acetaldehyde aqueous solution, $NaHCO_3$, ethanol, reflux; (c) HCHO, *N*-aliphatic amine, acetic acid, 30 ºC.

Target compounds **7a-7n** were prepared following the procedure outlined in Scheme 2. Acylation reaction of 1*H*-indole with acetic anhydride in the presence of anhydrous stannic chloride in nitromethane afforded 1-(1*H*-indol-3-yl)ethan-1-one **4** [28]. **4** was utilized in a convenient 4-component reaction with aromatic formaldehyde, malononitrile and ammonium acetate in refluxing toluene to give desired intermediates **5a-5b**, as was similar to the previously described protocol of **1a-1c** in scheme 1. Then, The entire imidazo[1,2-*a*]pyridine framework was packaged in one step with intermediates **5a-5b** in the presence of 1,3-dichloropropanone in ethanol giving rise to **6a-6b.** Eventually, nucleophilic substitution of the resultant **6a-6b** with appropriate *N*-aliphatic amines in refluxing ethanol afforded target compounds **7a-7n** in satisfied

yields.

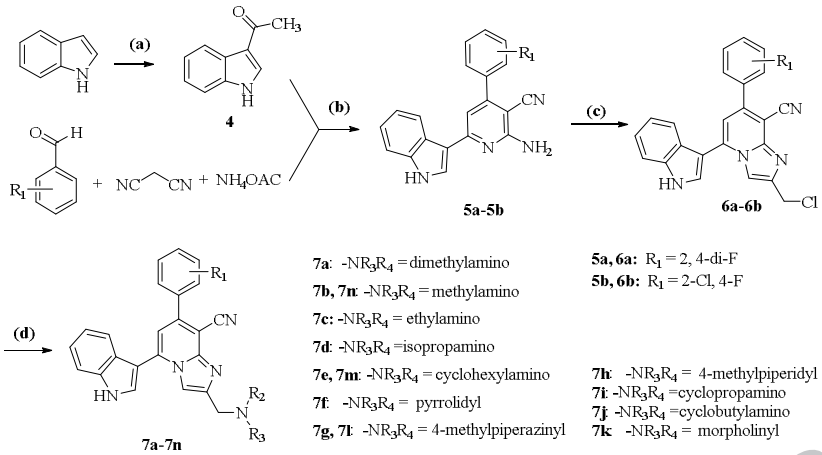

Scheme 2. Reagents and conditions: (a) acetic anhydride, anhydrous $SnCl_4$, nitromethane, 0 ℃ to r.t.; (b) toluene, reflux; (c) 1,3-dichloropropan-2-one, ethanol,reflux; (d) *N*-aliphatic amine, ethanol, reflux.

3. Results and discussions

3.1 Antiproliferative activity and SARs

To determine whether the imidazo[1,2-*a*]pyridine-8-carbonitrile skeleton is a suitable mimic for the *cis*-olefin presented in CA-4, two series of 5,7-diphenylimidazo[1,2-a]pyridine-8-carbonitrile derivatives (**3a-3q** and **7a-7n**) were examined for their cytotoxic activity against five cancer cells lines, HT29 (human colon cancer), H460 (human lung cancer), A549 (human lung carcinoma), MKN45 (human gastric cancer), and SMMC-7721 (human liver cancer) by a MTT assay. CA-4 and Crolibulin were used as the positive control. The results expressed as half-maximal inhibitory concentration (IC_{50}) values are depicted in Table 1-2, as mean values of experiments performed in triplicate.

Table 1. Cytotoxicity of **3a-3q** against HT29, H460, A549, MKN45 and SMMC-7721 cell lines *in vitro*.

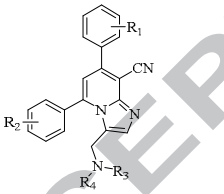

Compd.	R_1	R_2	$-NR_3R_4$	IC_{50}(μM) ±SD[a]				
				HT29	H460	A549	MKN45	SMMC-7721
3a	2,3,4-tri-OMe	4-F	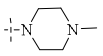	2.04±0.20	3.89±0.46	12.40±1.94	5.48±0.70	24.62±2.65
3b	2,3,4-tri-OMe	4-F		0.91±0.09	4.54±0.54	3.24±0.71	7.88±0.92	6.02±0.79
3c	2,3,4-tri-OMe	4-F		1.95±0.22	15.62±1.86	1.33±0.41	5.84±0.78	5.12±0.77
3d	2,3,4-tri-OMe	4-F		1.03±0.22	9.75±1.13	3.56±0.48	10.48±1.15	4.03±0.48
3e	2,3,4-tri-OMe	4-F		0.80±0.11	9.33±1.05	0.67±0.01	6.99±0.90	3.02±0.42

3f	2,3,4-tri-OMe	4-F		3.01±0.44	3.08±0.39	1.97±0.28	23.40±2.77	6.91±0.86
3g	2,3,4-tri-OMe	4-F		0.83±0.12	1.88±0.22	0.71±0.09	3.04±0.35	4.42±0.49
3h	2,3,4-tri-OMe	2,4-di-F		0.21±0.02	0.06±0.01	1.04±0.15	6.79±0.72	1.31±0.18
3i	2,3,4-tri-OMe	2,4-di-F		1.34±0.13	0.06±0.01	0.80±0.13	7.26±0.83	2.38±0.32
3j	2,3,4-tri-OMe	2,4-di-F		0.07±0.01	0.02±0.007	0.13±0.02	2.7±0.31	1.17±0.21
3k	2,3,4-tri-OMe	2,4-di-F		0.23±0.03	0.20±0.02	1.98±0.34	9.08±1.12	6.48±0.74
3l	2,3,4-tri-OMe	2,4-di-F		0.09±0.01	0.03±0.008	0.17±0.03	3.52±0.62	1.32±0.23
3m	2,3,4-tri-OMe	2,4-di-F		0.14±0.03	0.06±0.01	1.46±0.25	1.68±0.21	3.48±0.45
3n	2,3,4-tri-OMe	2,4-di-F		0.47±0.08	0.08±0.01	1.15±0.22	2.38±0.29	3.2±0.41
3o	3,4,5-tri-OMe	2,4-di-F		3.51±0.45	0.76±0.09	>100	40.57±5.03	>100
3p	3,4,5-tri-OMe	2,4-di-F		0.36±0.04	0.67±0.11	31.0±3.39	14.02±2.11	62.5±5.32
3q	3,4,5-tri-OMe	2,4-di-F		0.70±0.08	0.13±0.03	1.2±0.23	11.6±1.46	2.93±0.44
CA-4				0.05±0.01	0.08±0.01	0.43±0.053	0.11±0.02	1.92±0.11
Crolibulin				0.52±0.02[b]	0.03±0.01[b]	ND[b]	0.17±0.03[b]	ND[b]

[a] Data presented is the mean ± SD value of three independent determinations.

[b] reported IC_{50} value[22].

Table 2. Cytotoxicity of **7a-7q** against HT29, H460, A549, MKN45 and SMMC-7721 cell lines *in vitro*.

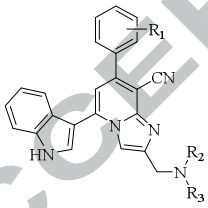

Compd.	R_1	$-NR_2R_3$	$IC_{50}(\mu M)\pm SD$[a]				
			HT29	H460	A549	MKN45	SMMC-7721
7a	2,4-di-F		0.06±0.008	0.19±0.02	1.12±0.16	1.34±0.21	5.30±0.62
7b	2,4-di-F		0.16±0.02	0.2±0.03	8.90±0.92	18.2±2.12	16.25±1.76
7c	2,4-di-F		0.05±0.06	0.15±0.02	0.92±0.94	2.77±0.34	6.12±0.68
7d	2,4-di-F		0.08±0.01	0.18±0.03	1.92±0.21	3.34±0.36	6.54±0.74

7e	2,4-di-F		0.01±0.002	0.04±0.006	0.54±0.06	2.4±0.28	5.6±0.56
7f	2,4-di-F		0.04±0.006	0.05±0.003	1.03±0.19	0.48±0.06	5.04±0.62
7g	2,4-di-F		0.11±0.01	0.17±0.02	0.92±0.09	2.71±0.32	3.82±0.48
7h	2,4-di-F	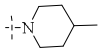	0.01±0.002	0.20±0.03	3.64±0.47	2.62±0.32	3.55±0.38
7i	2,4-di-F		0.04±0.009	0.28±0.04	9.66±1.02	3.68±0.45	6.8±0.72
7j	2,4-di-F		0.02±0.003	0.11±0.01	0.08±0.01	3.22±0.36	1.92±0.21
7k	2,4-di-F		2.7±0.27	0.19±0.02	3.33±0.42	7.86±0.85	12.84±1.34
7l	2-Cl, 4-F		0.14±0.02	0.22±0.03	1.55±0.18	3.62±0.38	7.12±0.76
7m	2-Cl, 4-F		0.02±0.004	0.08±0.01	2.53±0.26	3.68±0.42	4.88±0.53
7n	2-Cl, 4-F		0.12±0.01	0.25±0.03	1.04±0.15	2.44±0.26	5.66±0.87
CA-4			0.05±0.01	0.08±0.01	0.43±0.053	0.11±0.02	1.92±0.11
Crolibulin			0.52±0.02[b]	0.03±0.01[b]	ND[b]	0.17±0.03[b]	ND[b]

[a] Data presented is the mean ± SD value of three independent determinations.

[b] reported IC_{50} value[22].

As illustrated in Table 1, an expected observation was that most compounds showed moderate to excellent cytotoxic activity toward five tested cell lines, producing double-digit nanomolar IC_{50} values in some instances (e.g., analogues **3j, 3l, 7a, 7c, 7e, 7f, 7h-7j** and **7m**). Six compounds (**7e, 7f, 7h-7j** and **7m**) were optimized for their prominent antiproliferative activity with IC_{50} values ranging from 0.01 to 6.80 μM. Notably, the most promising compound **7e** displayed remarkable cytotoxicity whose IC_{50} values were 0.01 μM, 0.04 μM, 0.54 μM, 2.4 μM and 5.6 μM against HT29, H460, A549, MKN45 and SMMC-7721 cell lines respectively, which was 5-fold more potent than CA-4 and 52 times higher than Crolibulin selectively on HT29 cell, reflecting a good selectivity for colon cancer. As a general trend, the title compounds, especially for **7a-7n**, were more potent on HT-29 and H460 cells than on other cells. By contrast, the molecules displayed about 6- to 510-fold less sensitivity on SMMC-7721 cell as indicated by the IC_{50} values.

The pharmacological data disclosed a clear tendency related to the IMPs framework. As shown in Table 1, aromatic substituents (A and B ring) attached on IMPs skeleton plays a vital role in determining the cytotoxicity and selectivity of these inhibitors. To our surprise, introduction of 2,3,4-trimethoxyphenyl group at C-7 position of IMPs led to an obvious improvement in potency as compared with the relative 3,4,5-trimethoxyphenyl group (**3h** *vs.* **3o**, **3k** *vs.* **3p**,and **3i** *vs.* **3q**), as extend the modify limitation of A-ring restricted to 3,4,5-trimethoxyphenyl motif in CA-4. Moreover, replacement of 2,4-difluorophenyl group (R_2) at C-5 position (**3h-3n**) with 4-fluorophenyl moiety (**3a-3g**) resulted in a dramatic decrease in activity, indicating 2,4-difluoro

group is a favorable moiety in this region. For example, 2,4-difluorophenyl derivatives **3h** was approximate 3.4- to 51.4-fold more active than the corresponding 4-fluorophenyl analog **3f**.

Further structural optimization was conducted by introducing of diverse aliphatic aminomethyl groups on C-3 position of IMPs scaffold. The SARs based on IC_{50} values showed that variations of terminal aliphatic amino groups have a marked impact on activity. Interestingly, compound **3j** with the small methylamino motif exhibited the best activity against tested cells with IC_{50} values ranging from 0.07 to 2.7 μM, which was comparable to that of CA-4 and Crolibulin. By contrast, compounds **3m** (4-methylpiperidinyl) and **3i** (pyrrolidinyl) with bulky heterocyclic amino groups demonstrated an approximate 2- to 19-fold diminished potency against tested cells**,** except for on MKN-45. Accordingly, secondary amino derivatives, such as **3j** (HT-29, IC_{50} = 0.07 μM) and **3l** (HT-29, IC_{50} = 0.09 μM)**,** exhibited better cytotoxicity than tertiary amino derivatives **3h** (HT-29, IC_{50} = 0.21 μM)**, 3i** (HT-29, IC_{50} = 1.34 μM) and **3k** (HT-29, IC_{50} = 0.23 μM). The loss in activity might be due to the steric clash between alkylamino chain and aryl B-ring which prevent the test molecule from reaching the colchicine binding site of tubulin. The same trend was observed among compounds **3a**-**3g**.

To further optimize structural skeleton, we prepared a series of 5-indolyl-7-arylimidazo[1,2-*a*]pyridine-8-carbonitrile derivatives **7a-7n** by introducing diverse *N*-aliphatic amino groups into the C-2 position on IMP skeleton. Inspired by the outstanding cytotoxicity of **3j**, the favorable 2,4-difluorophenyl group was introduced to C-7 position producing analogs **7a-7k**. Additionally, **7l-7n** with 2-chloro-4-flourophenyl moiety were synthesized to explore the extending SARs. It is worth noting that embedment of indolyl group turned out to enhance the antiproliferative potency as compared with the relative phenyl derivatives **3a-3q**, in good agreement with the low expand ability and of the B ring pocket at the colchicine site. Meanwhile, replacement of 2,4-diflourophenyl group (R_1) with 2-chloro-4-flourophenyl (**7l, 7m** and **7n**) altered cytotoxicity slightly, indicating that halogen at phenyl R_1 fragment contributed little to potency.

The data presented in Table 2 indicated that the cytotoxicity of **7a-7n** was generally higher than the corresponding **3a-3q**, suggesting that the substituted amino group at C-2 position is favor for activity. Interestingly, an altered or even reverse trend was observed when the aliphatic amino groups were shifted from C-3 to C-2 position on IMP skeleton. Differ from **3j**, compound **7b** with tiny methylamino group displayed poor potency as compared to others. Contrary to **3a-3q,** compounds bearing secondary amino (e.g. methyl group, ethyl group, isopropyl group) indicated 1.2- to 16-fold decrease in potency than tertiary alicyclic amino analogs (e.g. cyclehexyl, 4-methylpiperidinyl and pyrrolidinyl) as comparison of **7a** and **7b**, **7d** and **7f**. To our delight, 2-((cyclohexylamino)methyl)-7-(2,4-difluorophenyl)-5-(1*H*-indol-3-yl)imidazo[1,2-*a*]pyridine-8-carbonitrile **7e** exhibited prominent cytotoxicity whose IC_{50} value ranging from 0.01 to 6.80 μM, superior to positive control and other analogs. However, a dramatic loss in cytotoxic potency was observed for derivatives **7g** (HT-29, IC_{50} = 0.11 μM) or **7k** (HT-29, IC_{50} = 2.7 μM) with 4-methylpiperizino or morpholino groups respectively, indicating the heterocyclic amino was not favorable for this region. Additional SARs and further optimization are in progress and will be reported in due course.

3.2 7e disturbs microtubule polymerization

To further ascertain the promising cytotoxic potency of the target compounds are due to

interference with the mitotic machinery, we analyzed the antitubulin effect of the lead **7e** on cellular microtubule networks *via* tubulin immunofluorescence in HT29 cells [29]; CA-4 was tested for comparison. As shown in Fig. 2, the immunofluorescence analysis using the specific antibodies to *α*-tubulin revealed that the microtubule network of the cells in negative control group was homogenous, intact arranged and well organized. However, cells exposed to either CA-4 (20 nM) or **7e** (88 nM) for 24 h induced abnormal microtubule network arrangement and exhibited cellular microtubule depolymerization with scattered short microtubule fragments in the cytoplasm of HT-29 cells. The results confirm that tubulin polymerization was disturbed by **7e**, indicating the potential tubulin-targeted activity possessed by this lead compound.

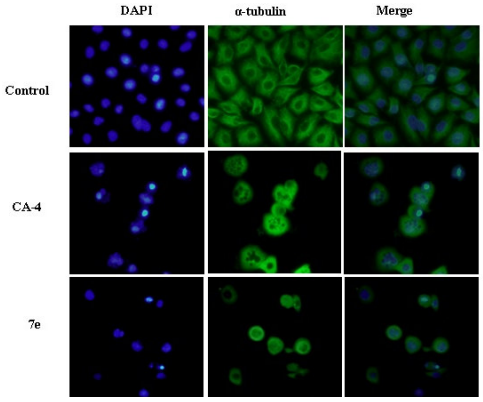

Figure 2. Immunofluorescence assay on **7e** in HT29 cells. HT29 cells were treated with CA-4 (20nM) or **7e** (88 nM) for 24 h. After incubation, the cells were fixed, stained with monoclonalα-tubulin antibody (green) at 4 ℃ overnight and then reacted with FITCconjugatedsecondary antibody. DAPI (blue) was used for nuclear counterstaining. The cellular microtubules were observed by fluorescence microscopy (*scalebar* = 20 μm).

3.3 7e binds to tubulin at the colchicine site.

These IMP derivatives showed similar inhibitory effects on tubulin assembly to that of CA-4 and which prompted us to investigate whether **7e** bind to the colchicine site of the tubulin by employing fluorescence based colchicine binding assay in parallel with CA-4 and Taxol as reference [30]. It was observed that at low concentration the test compound **7e** and CA-4 showed significant affinity towards colchicine site, whereas at higher concentrations both of them showed more binding affinity as shown in Fig. 3. The decrease in fluorescence of the colchicine-tubulin complex in the presence of **7e** was in a dose‑dependent manner site on tubulin. The taxol was used as a negative control, which is known to binding at different site and shows no effect on tubulin-colchicine complex [31]. Therefore, the results supported a notion that **7e** binds to the colchicine site on tubulin although inferior to CA-4.

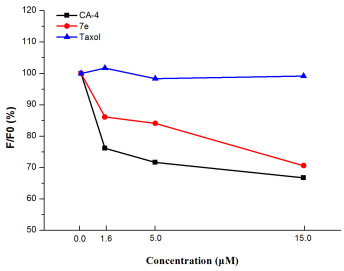

Figure 3. Fluorescence based colchicine competitive binding assay on **7e.** Tubulin was co-incubated with

indicated concentrations of Taxol, **7e** or CA-4 for 1 h, and then 5 μmol/L colchicine was added. The fluorescence was measured by Hitachi F-2500 spectrofluorometer.

3. 4 Molecular modeling analysis

A molecular docking study was conducted to elucidate the hypothetical binding mode of 5,7-diarylimidazo[1,2-*a*]pyridine-8-carbonitrile derivative **7e** that exhibited potent cytotoxic activity in the colchicine-binding site cavity using Discovery Studio Program 3.5. The surflex-Dock program in Sybyl-X 2.1.1 was used to dock **7e** into the colchicine-binding site of tubulin following the removal of the ligand from the 3D crystal structure of the DAMA-colchicines-tubulin complex (PDB code: 4O2B) [32].

According to the docking model, **7e** occupied the colchicine binding site of tubulin (Fig.4B/C). Most of all, the cyano group on IMPs skeleton formed a strong hydrogen bond with the amino group of Asn249 of *β*-tubulin and inferior Pi-donor hydrogen bond with protein residue Leu248. Moreover, the IMP framework could also generate several alkyl interactions by linking up to Ala180, Ala354, Lys352 and Leu248 (Fig. 4A), suggesting introduction of IMPs scaffold could foster potent tubulin-binding affinity leading to significant antiproliferative activities. And also, the phenyl and indolyl groups were involved in the alkyl, Pi-donor hydrogen bond and halogen interactions (Fig. 4A). Concretely, the diflourophenyl moiety could form hydrophobic interactions with the hydrophobic pocket made up by Ala250, Thr179, Asn101, Gly143 and Ser178. Significantly, the fluorine at C-2 position forms halogen interaction well with Asn249, as may be the reason that introducing halogen groups could enhance the antitubulin activity. Meanwhile, a Pi-sulfur interaction between the indolyl group and Met 259 residue, and a few alkyl interactions with Ala180 and Lys352 were formed successively. In addition, the cyclohexyl moiety was responsible for the hydrophobic and alkyl interactions with Ala317, Ile378 and Ile 318. Notably, the overlapped 3D model of candidate **7e** and Crolibulin (Fig.4D) indicated that **7e** was oriented in the similar manner with matching occupancy at the colchicine-binding site of tubulin. Thus, the results from the docking study were in accordance with the SARs analysis.

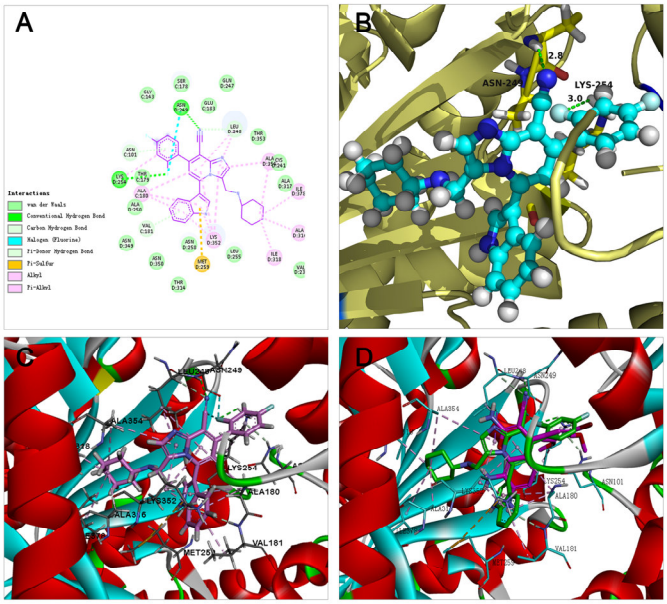

Figure 4.The binding mode between the active conformation of **7e** and tubulin. (A) 2D diagram of the interaction between **7e** and colchicine-binding site.(B/C)3D diagram of the interaction between **7e** and colchicine-binding site.

For clarity, only interacting residues are displayed. The H-bond (green arrows) is highlighted as dotted arrows in 4B. (D)Predicted modes for **7e**(green) and Crolibulin (pink) binding at the colchicine-binding site of tubulin (PDB code: 4O2B), and overlapping with each other.

4. Conclusions

Imidazo[1,2-*a*]pyridine-8-carbonitriles serving as the "privileged medicinal scaffolds" are of particular utility for generation of small-molecule ligands with pronounced antitumor efficacy. Herein, with an aim to develop antitubulin agents targeting colchicine-binding site, we discovered two series of 5,7-diarylimidazo[1,2-*a*]pyridine-8-carbonitrile derivatives (**3a-3q** and **7a-7n**) according to bioisosterism and hybridization principles. All the compounds were prepared *via* a concise three-step process involving acylation reaction, one-pot coupling reaction and cyclization transformation, and their antiproliferative activities were evaluation against a panel of human cancer cell lines (HT29, H460, A549, MKN-45, and SMMC-7721) in MTT assay. The preliminary investigation showed that several molecules (e.g. **3j, 3l, 7e, 7f, 7h-7j** and **7m**) displayed promising cytotoxic activity with IC_{50} values in a double-digit nanomolar range. Optimization towards these series of compounds resulted in the discovery of **7e**, which displayed noteworthy antitumor potency with IC_{50} value of 0.01 μM, 0.04 μM, 0.54 μM, 2.4 μM, and 5.6 μM against HT29, H460, A549, MKN45 and SMMC-7721 cell lines respectively, superior to positive CA-4 and Crolibulin on most of the tested cells. The preliminary SARs provided a useful insight that could be utilized in developing improved leads based on IMPs skeleton. Notably, fluorescence based colchicine competitive binding assay as well as immunofluorescence assay were undertook which demonstrated that tubulin polymerization was disturbed by **7e** by binding at colchicine site of tubulin. Moreover, a docking mode revealed that **7e** could foster potent tubulin-binding affinity by forming critical hydrogen bonding and hydrophobic interactions, and orient in the similar manner with Crolibulin occupied at the colchicine-binding site in overlap 3D model, in good agreement with the pharmacological activity and the observed SARs for these series of compounds.

In summary, the SARs-guided discovery process and docking models led to identify a candidate **7e**, which could provide helpful guidance in development of new chemical entities as effective colchicines-binding-site targeted tubulin polymerization inhibitors.

5. Experimental protocols

5.1 Chemistry

All melting points were obtained on a Büchi Melting Point B-540apparatus (BüchiLabortechnik, Flawil, Switzerland) and were uncorrected.Mass spectra (MS) were taken in ESI mode on Agilent100 LC-MS (Agilent, Palo Alto, CA, USA). ^{1}H NMR and ^{13}C NMR spectroscopy was performed using Bruker ARX-400 and ARX-600spectrometers (Bruker Bioscience, Billerica, MA, SA) with TMS as an internal standard. Column chromatography was run on silica gel (200-300 mesh) from Qingdao Ocean Chemicals (Qingdao, Shandong, China). Unless otherwise noted, all materials were obtained from commercially available sources and were used without further purification.

*5.1.1. General procedure for preparation of 2-amino-4,6-diarylnicotinonitrile (**1a-1c**)*

To a solution of aromatic formaldehydes (0.1mol) in toluene (300 mL) was added substituted acetophenones (0.1mol), malononitrile (6.6 g, 0.1 mol) and ammonium acetate (61.6 g, 0.8mol). The reaction mixture was refluxed for 8 h. Upon cooling to room temperature, the solvent was evaporated under *vacuum* and the residue was triturated with ethanol (150 mL). After stirring for

10 min, the resulting precipitant was filtered, and the filtrate was further stirred with ethanol (200 mL) overnight. Thus, the resultant solid were collected by filtration to afford compounds **1a-1c**.

*5.1.1.1. 2-amino-6-(4-fluorophenyl)-4-(2,3,4-trimethoxyphenyl)nicotinonitrile (**1a**)*

Pale yellow solid.Yield: 51.3%. MS (ESI) m/z (%): 380.2 $[M+H]^+$.

*5.1.1.2. 2-amino-6-(2,4-difluorophenyl)-4-(2,3,4-trimethoxyphenyl)nicotinonitrile (**1b**)*

Pale yellow solid.Yield: 46.5%. MS (ESI) m/z (%):398.2 $[M+H]^+$.

*5.1.1.3. 2-amino-6-(2,4-difluorophenyl)-4-(3,4,5-trimethoxyphenyl)nicotinonitrile (**1c**)*

Pale yellow solid.Yield: 41.9%. MS (ESI) m/z (%): 398.2 $[M+H]^+$.

*5.1.2. General procedure for preparation of 5,7-diarylimidazo[1,2-a]pyridine-8-carbonitrile (**2a-2c**)*

A mixture of 2-amino-4,6-diarylnicotinonitrile (**1a-1c**) (46.1 mmol), 40% acetaldehyde aqueous solution (90 mL, 46.1 mmol), sodium bicarbonate (7.7 g, 92.2 mmol) in ethanol (180 mL) was heated to reflux and stirred for 7 h, whereby a yellow suspension was formed. After completion of the reaction indicated by TLC, the mixture was cooled to room temperature, and the solvent was evaporated under reduced pressure. The residue was dissolved in the mixture solution of H_2O/CH_2Cl_2 (1:1, 400 mL) and stirred for 10 min, and the aqueous layer was extracted with CH_2Cl_2 twice. The combined organic layer was washed with water (200 mL×2) and brine, dried over anhydrous Na_2SO_4 and concentrated *in vacuum*. The residue was triturated with isopropyl ether (150 mL) for 1 h, and the solid were filtered and air-dried to furnish compounds **2a-2c**.

*5.1.2.1. 5-(4-fluorophenyl)-7-(2,3,4-trimethoxyphenyl)imidazo[1,2-a]pyridine-8-carbonitrile (**2a**)*

Pale while solid. Yield: 74.4%. MS (ESI) m/z (%):404.2 $[M+H]^+$.

*5.1.2.2. 5-(2,4-difluorophenyl)-7-(2,3,4-trimethoxyphenyl)imidazo[1,2-a]pyridine-8-carbonitrile (**2b**)*

Pale while solid. Yield: 82.7%. MS (ESI) m/z (%):422.2 $[M+H]^+$.

*5.1.2.3. 5-(2,4-difluorophenyl)-7-(3,4,5-trimethoxyphenyl)imidazo[1,2-a]pyridine-8-carbonitrile (**2c**)*

Pale while solid. Yield: 79.1%. MS (ESI) m/z (%):422.2 $[M+H]^+$.

*5.1.3. General procedure for preparation compounds (**3a-3q**)*

To a mixture of 37% formalin (3.6 mmol) in acetic acid (15 mL) was added various *N*-aliphatic amine (3.6 mmol). After stirring for 30 min, **2a-2c** (1.2 mmol) was added at room temperature. Until dissolved completely, the solution was heat to 30ºC and stirred. After completion of the reaction monitored by TLC, the solution was cooled to room temperature, and poured into water (50 mL).Insoluble residues were removed by filtration, and the filtrate was basified with ammonium hydroxide (25%) to pH 8. The resulting precipitate was filtered, dried to give crude products. The crude products was purified by chromatography on silica gel using CH_2Cl_2/MeOH (20:1) to afford the desired compounds **3a-3q**.

*5.1.3.1. 5-(4-fluorophenyl)-3-((4-methylpiperazin-1-yl)methyl)-7-(2,3,4-trimethoxyphenyl)imidazo [1,2-a]pyridine-8-carbonitrile (**3a**)*

White solid.Yield:95.8%.m.p.: 189.3-190.8 ºC. MS(ESI) m/z(%):516.2 $[M+H]^+$. ^1H NM R (400 MHz, $CDCl_3$) δ: 7.59 (s, 1H), 7.47 (dd, J = 7.8, 5.5 Hz, 2H), 7.19–7.11 (m, 3H), 6.76 (t, J = 4.2 Hz, 2H), 3.88 (d, J = 3.8 Hz, 6H), 3.81 (s, 3H), 3.22 (s, 2H), 1.95 (m, 2H), 2.69 (m, 2H), 2.50 (m, 2H), 2.29 (m, 2H), 2.12 (s, 3H).Anal. calcd. for $C_{29}H_{30}FN_5O_3$ (%):C, 67.56, H, 5.87, N, 13.58. Found (%):C, 67.51, H, 5.78, N, 13.52.

*5.1.3.2. 3-((ethylamino)methyl)-5-(4-fluorophenyl)-7-(2,3,4-trimethoxyphenyl)imidazo[1,2-a]pyridine-8-carbonitrile (**3b**)*

White solid.Yield:93.6%.m.p.: 195.2-197.0ºC. MS(ESI) m/z(%):461.1 $[M+H]^+$.^{1}H NMR (400 MHz, $CDCl_3$) δ: 7.59 (s, 1H), 7.47 (dd, J = 7.8, 5.5 Hz, 2H), 7.19 –7.11 (m, 3H), 6.76 (t, J = 4.2 Hz, 2H), 3.88 (d, J = 3.8 Hz, 6H), 3.81 (s, 3H), 3.22 (s, 2H), 2.49 (m, 1H), 1.84 (m, 1H), 1.35 (s, 1H), 1.19 (t, J = 5.1 Hz, 3H).Anal.calcd. for $C_{26}H_{25}FN_4O_3$ (%):C, 67.81, H, 5.47, N, 12.17. Found (%):C, 67.76, H, 5.39, N, 12.12.

*5.1.3.3. 5-(4-fluorophenyl)-3-(pyrrolidin-1-ylmethyl)-7-(2,3,4-trimethoxyphenyl)imidazo[1,2-a]pyridine-8-carbonitrile (**3c**)*

White solid.Yield: 89.1%. m.p.: 176.5-179.0 ºC. MS(ESI) m/z(%):487.2 $[M+H]^+$.^{1}H NMR (400 MHz, $CDCl_3$) δ: 7.60 (s, 1H), 7.49 (dd, J = 7.8, 5.5 Hz, 2H), 7.22 –7.10 (m, 3H), 6.76 (t, J = 4.2 Hz, 2H), 3.88 (d, J= 3.8 Hz, 6H), 3.82 (s, 3H), 3.23 (s, 2H), 2.00 (s, 4H), 1.56 (s, 4H). Anal.calcd. for$C_{28}H_{27}FN_4O_3$ (%):C, 69.12, H, 5.59, N, 11.52. Found (%): C, 69.07, H, 5.52, N,11.46.

*5.1.3.4. 5-(4-fluorophenyl)-3-(morpholinomethyl)-7-(2,3,4-trimethoxyphenyl)imidazo[1,2-a]pyridine-8-carbonitrile (**3d**)*

White solid.Yield:77.8%.m.p.: 170.0-171.6ºC. MS(ESI) m/z(%):503.0 $[M+H]^+$. ^{1}H NMR (400 MHz, $CDCl_3$) δ: 7.61 (s, 1H), 7.51 (dd, J = 8.5, 5.2 Hz, 2H), 7.18 (dd, J= 17.2, 8.6 Hz, 3H), 6.83 – 6.73 (m, 2H), 3.90 (d, J= 4.9 Hz, 6H), 3.85 (s, 3H), 3.43 (s, 4H), 3.17 (s, 2H), 1.93 – 1.80 (m, 4H).Anal.calcd. for$C_{28}H_{27}FN_4O_4$ (%):C, 66.92, H, 5.42, N, 11.15. Found (%):C, 66.84, H, 5.37, N, 11.07.

*5.1.3.5. 3-((dimethylamino)methyl)-5-(4-fluorophenyl)-7-(2,3,4-trimethoxyphenyl)imidazo[1,2-a]pyridine-8-carbonitrile (**3e**)*

White solid.Yield:91.9%.m.p.: 147.5-149.0ºC. MS(ESI) m/z(%):461.2 $[M+H]^+$. ^{1}H NMR (400 MHz, $CDCl_3$) δ: 7.59 (s, 1H), 7.47 (dd, J = 7.8, 5.5 Hz, 2H), 7.19 –7.11 (m, 3H), 6.76 (t, J= 4.2 Hz, 2H), 3.88 (d, J= 3.6 Hz, 6H), 3.81 (s, 3H), 3.22 (s, 2H), 2.29 (s, 6H).Anal.calcd. for $C_{26}H_{25}FN_4O_3$ (%):C, 67.81, H, 5.47, N, 12.17. Found (%):C, 67.74, H, 5.41, N, 12.11.

*5.1.3.6. 3-((diethylamino)methyl)-5-(4-fluorophenyl)-7-(2,3,4-trimethoxyphenyl)imidazo[1,2-a]pyridine-8-carbonitrile (**3f**)*

White solid.Yield:83.2%. m.p.: 119.2-121.0 ºC. MS(ESI) m/z(%): 489.2 $[M+H]^+$.^{1}H NMR (400 MHz, $CDCl_3$) δ: 7.66 (s, 1H), 7.47 (dd, J = 7.8, 5.5 Hz, 2H), 7.21 – 7.12 (m, 3H), 6.76 (d, J= 4.2 Hz, 2H), 3.88 (d, J = 3.8 Hz, 6H), 3.80 (s, 3H), 3.27 (s, 2H), 2.16 – 2.00 (m, 4H), 0.71 (t, J= 7.0 Hz, 6H).Anal.calcd. for$C_{28}H_{29}FN_4O_3$(%):C, 68.84, H, 5.98, N, 11.47. Found (%):C, 68.78, H, 5.94, N, 11.43.

*5.1.3.7. 5-(4-fluorophenyl)-3-((methylamino)methyl)-7-(2,3,4-trimethoxyphenyl)imidazo[1,2-a]pyridine-8-carbonitrile (**3g**)*

White solid. Yield: 74.7%.m.p.: 152.4-153.9 ºC. MS(ESI) m/z(%):447.0 $[M+H]^+$. ^{1}H NMR (400 MHz, $CDCl_3$) δ: 7.79 (s, 1H), 7.61 (dd, J = 8.3, 5.2 Hz, 2H), 7.27 – 7.18 (m, 3H), 6.84 (s, 1H), 6.79 (d, J= 8.8 Hz, 1H), 3.91 (d, J= 4.9 Hz, 6H), 3.81 (s, 3H), 3.47 (s, 3H), 2.15 (s, 3H).Anal.calcd. for$C_{25}H_{23}FN_4O_3$(%):C, 67.25, H, 5.19, N, 12.55. Found (%): C, 67.19, H, 5.14, N, 12.50.

*5.1.3.8.3-((diethylamino)methyl)-5-(2,4-difluorophenyl)-7-(2,3,4-trimethoxyphenyl)imidazo[1,2-a]pyridine-8-carbonitrile (**3h**)*

White solid.Yield:77.8%.m.p.: 149.1-150.7ºC. MS(ESI) m/z(%):533.3 $[M+H]^+$. ^1H NMR (400 MHz, $CDCl_3$) δ: 7.66 (s, 1H), 7.58 (dd,*J*= 14.3, 7.6 Hz, 1H), 7.24 (d, *J*= 8.7 Hz, 1H), 7.02 (td, *J* = 8.1, 1.9 Hz, 1H), 6.95 (td, *J* = 9.1, 2.4 Hz, 1H), 6.85 (s, 1H), 6.79 (d, *J* = 8.7 Hz, 1H), 3.92 (s, 3H), 3.88 (s, 6H), 3.08 (s, 2H), 2.55 (m, 4H), 1.05 (t, *J* = 5.1 Hz, 6H).Anal.calcd. for $C_{28}H_{28}F_2N_4O_3$ (%):C, 66.39, H, 5.57, N, 11.06. Found (%):C, 66.35, H, 5.55, N, 11.02.

*5.1.3.9. 5-(2,4-difluorophenyl)-3-(pyrrolidin-1-ylmethyl)-7-(2,3,4-trimethoxyphenyl)imidazo[1,2-a]pyridine-8-carbonitrile (**3i**)*

White solid.Yield:83.9%.m.p.: 189.3-190.8 ºC. MS(ESI) m/z(%):531.1 $[M+H]^+$. ^1H NMR (400 MHz, $CDCl_3$) δ: 7.66 (s, 1H), 7.48 (dd, *J* = 14.3, 7.6 Hz,1H), 7.24 (d, *J* = 8.7 Hz, 1H), 7.02 (td, *J* = 8.1, 1.9 Hz, 1H), 6.95 (td, *J* = 9.1, 2.4 Hz, 1H), 6.85 (s, 1H), 6.79 (d, *J* = 8.7 Hz, 1H), 3.92 (s, 3H), 3.88 (s, 6H), 3.08 (s, 2H),3.02 (m, 2H), 2.36 (m, 2H), 1.56 (s, 4H).Anal.calcd. for $C_{28}H_{26}F_2N_4O_3$ (%):C, 66.66, H, 5.19, N, 11.10. Found (%):C, 66.64, H, 5.11, N, 11.05.

*5.1.3.10. 5-(2,4-difluorophenyl)-3-((methylamino)methyl)-7-(2,3,4-trimethoxyphenyl)imidazo[1,2-a]pyridine-8-carbonitrile (**3j**)*

White solid. Yield: 90.9%.m.p.: 132.4-134.2ºC. MS(ESI) m/z(%):491.4 $[M+H]^+$.^1H NMR (400 MHz, $CDCl_3$)δ: 7.60 (s, 1H), 7.48 (d, *J* = 6.0 Hz, 1H), 7.24 (d, *J* = 8.7 Hz, 1H), 7.03 – 6.97 (m, 1H), 6.95 (d, *J* = 8.7 Hz, 1H), 6.85 (s, 1H), 6.79 (d, *J* = 8.7 Hz, 1H), 3.91 (d, *J* = 3.8 Hz, 6H), 3.82 (s, 3H), 3.13 (d, *J* = 4.4 Hz, 2H), 2.15 (s, 3H). Anal.calcd.for $C_{25}H_{22}F_2N_4O_3$(%):C, 64.65, H, 4.77, N, 12.06. Found(%): C, 64.57, H, 4.68, N, 12.00.

*5.1.3.11. 5-(2,4-difluorophenyl)-3-((dimethylamino)methyl)-7-(2,3,4-trimethoxyphenyl)imidazo[1,2-a]pyridine-8-carbonitrile (**3k**)*

White solid.Yield:87.4%.m.p.: 152.1-155.0 ºC. MS(ESI) m/z(%):479.3 $[M+H]^+$.^1H NMR (400 MHz, $CDCl_3$) δ: 7.63 (s, 1H), 7.48 (dd, *J* = 14.3, 7.6 Hz, 1H), 7.24 (d, *J* = 8.7 Hz, 1H), 7.02 (td, *J* = 8.1, 1.9 Hz, 1H), 6.95 (td, *J* = 9.1, 2.4 Hz, 1H), 6.85 (s, 1H), 6.79 (d, *J* = 8.7 Hz, 1H), 3.91 (d, *J* = 3.8 Hz, 6H), 3.82 (s, 3H), 3.20-3.07 (m, 2H), 1.75 (s, 6H).Anal.calcd. for$C_{26}H_{24}F_2N_4O_3$ (%):C, 65.26, H, 5.06, N, 11.71. Found (%):C, 65.23, H, 4.99, N, 11.66.

*5.1.3.12. 5-(2,4-difluorophenyl)-3-((ethylamino)methyl)-7-(2,3,4-trimethoxyphenyl)imidazo[1,2-a]pyridine-8-carbonitrile (**3l**)*

White solid.Yield: 97.4%.m.p.: 162.1-163.8 ºC. MS(ESI) m/z(%):505.2 $[M+H]^+$.^1H NMR (400 MHz, $CDCl_3$) δ: 7.59 (s, 1H), 7.44 (dd, *J* = 14.3, 7.6 Hz, 1H), 7.26 (d, *J* = 8.8 Hz, 1H), 7.04 – 6.91 (m, 2H), 6.85 (s, 1H), 6.78 (d, *J* = 8.8 Hz, 1H), 3.91 (d, *J* = 3.4 Hz, 6H), 3.82 (s, 3H), 3.16 (dd, *J* = 26.1, 13.2 Hz, 2H),2.69 (m, 1H), 2.19 (m, 1H), 1.48 (s, 1H), 1.20 (t, *J* = 5.0 Hz, 3H).Anal.calcd. for $C_{26}H_{24}F_2N_4O_3$ (%): C, 65.26, H, 5.06, N, 11.71. Found (%):C, 65.23, H, 4.99, N, 11.66.

*5.1.3.13. 5-(2,4-difluorophenyl)-3-((4-methylpiperidin-1-yl)methyl)-7-(2,3,4-trimethoxyphenyl)imidazo[1,2-a]pyridine-8-carbonitrile (**3m**)*

White solid.Yield:92.1%.m.p.: 193.3-197.1 ºC. MS(ESI) m/z(%):533.1 $[M+H]^+$. ^1H NMR (400 MHz, $CDCl_3$) δ: 7.59 (s, 1H), 7.44 (d, *J* = 5.9 Hz, 1H), 7.24 (d, *J* = 8.8 Hz, 1H), 7.03 – 6.97 (m, 1H), 6.94 (d, *J*=8.7 Hz, 1H), 6.85 (s, 1H), 6.78 (d, *J* = 8.6 Hz, 1H), 3.91 (d, *J* = 3.4 Hz, 6H), 3.82 (s, 3H), 3.16 (dd, *J* = 26.8, 13.9 Hz, 2H), 2.01 (d,*J*=0.6

Hz, 2H), 1.59 (d, *J* = 9.6 Hz, 2H), 1.39 (d, *J* = 11.5 Hz, 2H), 1.23 (d, *J* = 12.8 Hz, 3 H), 0.83 (d, *J* = 6.3 Hz, 3H).Anal.calcd. for$C_{30}H_{30}F_2N_4O_3$ (%):C, 67.66, H, 5.68, N, 10.52. Found (%):C, 67.61, H, 5.64, N, 10.47.

*5.1.3.14. 5-(2,4-difluorophenyl)-3-(morpholinomethyl)-7-(2,3,4-trimethoxyphenyl)imidazo[1,2-a] pyridine-8-carbonitrile (**3n**)*

White solid.Yield:69.9%.m.p.: 149.1-150.6 ºC. MS(ESI) m/z(%):521.0 $[M-H]^+$.^{1}H NMR (400 MHz, $CDCl_3$) δ: 8.16 (td, *J* = 8.9, 6.7 Hz, 1H), 7.90 (d, *J* = 1.1 Hz, 1H), 7.12 (d, *J* = 8.6 Hz, 2H), 7.03 (td, *J* = 8.2, 2.1 Hz, 1H), 6.95 (ddd, *J* = 11.3, 8.6, 2.4 Hz, 1H), 6.81 (d, *J* = 8.7 Hz, 1H), 6.30 (t, *J* = 3.1 Hz, 1H), 6.27 (s, 1H), 3.94 (s, 6H), 3.93 (s, 3H), 3.71 (s, 2H), 3.34 (s, 3H), 2.19 (s, 3H).Anal.calcd. for$C_{28}H_{26}F_2N_4O_4$ (%):C, 64.61, H, 5.03, N, 10.76. Found (%):C, 64.54, H, 4.97, N, 10.67.

*5.1.3.15.3-((diethylamino)methyl)-5-(2,4-difluorophenyl)-7-(3,4,5-trimethoxyphenyl)imidazo[1,2-a]pyridine-8-carbonitrile (**3o**)*

White solid.Yield:66.0%.m.p.: 173.0-174.7 ºC. MS(ESI) m/z(%):507.0 $[M+H]^+$.^{1}H NMR (400 MHz, $CDCl_3$) δ: 7.66 (s, 1H), 7.58 (td, *J* = 8.5, 6.3 Hz, 1H), 7.07 – 6.96 (m, 2H), 6.81 (d, *J*= 1.3 Hz, 1H), 6.75 (s, 2H), 3.92 (s, 3H), 3.88 (s, 6H), 3.10 (s, 2H),2.75 (m, 2H), 2.54 (m, 2H), 1.01 (t, *J* = 5.1 Hz, 6H).Anal.calcd. for $C_{28}H_{28}F_2N_4O_3$ (%):C, 66.39, H, 5.57, N, 11.06.Found (%):C, 66.33, H, 5.55, N, 10.98.

*5.1.3.16.5-(2,4-difluorophenyl)-3-((dimethylamino)methyl)-7-(3,4,5-trimethoxyphenyl)imidazo[1,2-a]pyridine-8-carbonitrile (**3p**)*

White solid.Yield:87.2%.m.p.: 143.7-145.8 ºC. MS(ESI) m/z(%):479.1 $[M+H]^+$.^{1}H NMR (400 MHz, $CDCl_3$) δ: 7.66 (s, 1H), 7.58 (td, *J* = 8.5, 6.3 Hz, 1H), 7.07 – 6.96 (m, 2H), 6.81 (d, *J* = 1.3 Hz, 1H), 6.75 (s, 2H), 3.92 (s, 3H), 3.88 (s, 6H), 3.10 (s, 2H), 1.86 (s, 6H).Anal.calcd. for $C_{26}H_{24}F_2N_4O_3$ (%):C, 65.26, H, 5.06, N, 11.71. Found (%):C, 65.23, H, 4.99, N, 11.66.

*5.1.3.17.5-(2,4-difluorophenyl)-3-(pyrrolidin-1-ylmethyl)-7-(3,4,5-trimethoxyphenyl)imidazo[1,2-a]pyridine-8-carbonitrile (**3q**)*

White solid.Yield: 92.0%.m.p.: 189.3-190.8 ºC. MS(ESI) m/z(%):531.1 $[M+H]^+$.^{1}H NMR (400 MHz, $CDCl_3$) δ: 7.66 (s, 1H), 7.58 (td, *J* = 8.5, 6.3 Hz, 1H), 7.07 – 6.96 (m, 2 H), 6.81 (d, *J* = 1.3 Hz, 1H), 6.75 (s, 2H), 3.92 (s, 3H), 3.88 (s, 6H), 3.10 (s, 2H), 3.02 (m, 2H), 2.33 (m, 2H), 1.70 (m, 4H).Anal.calcd. for $C_{28}H_{26}F_2N_4O_3$ (%):C, 66.66, H, 5.19, N, 11.10. Found (%):C, 66.59, H, 5.12, N, 11.04.

*5.1.4. Preparation of 1-(1H-indol-3-yl)ethan-1-one (**4**)*

A 500mL oven-dried three-necked flask was dealed with septa and backfilled with nitrogen gas (N_2) three times before starting the reaction.To a stirring solution of indole (23.4 g, 0.2 mol) in CH_2Cl_2 (200 mL), a suspension of anhydrous $SnCl_4$ (62.4g, 0.24 mol) in dried CH_2Cl_2 (150 mL) was dropped, and the mixture was stirring at 0 ºC for 30 min. Then acetic anhydride (15.5 g, 0.2 mol) in CH_2Cl_2 (100 mL) was added dropwise. Upon the completion of reaction, a brown nitromethane (50 mL) solvent was added slowly, and the mixture was stirred at 0 ºC for 30 min. Then the mixture was warmed to room temperature and further stirred for 2 h. After being quenched with ice aqueous solution (30 mL), the suspension solution was filtered and the filtrate was extracted with ethyl acetate twice (100 mL×2). The combined organic phase was washed with water and brine, then dried overNa_2SO_4 and concentrated at reduced pressure to give a dark brown solid. The solid was triturated with ethanol (100 mL) for 1 h, and collected by filtration to

generate **4** as an off white solid in 79.3%yield. MS (ESI) m/z (%):160.1[M+H]$^+$.

*5.1.5. General procedure for preparation of 2-amino-6-(1H-indol-3-yl)-4-arylnicotinonitrile (**5a-5b**)*

To a solution of substituted benzaldehyde (0.1mol) in toluene (250 mL) was added 1-(1*H*-indol-3-yl)ethan-2-one **4** (9.1 mL, 0.1 mol), malononitrile (6.6 g, 0.1 mol) and ammonium acetate (61.6 g, 0.8 mol) at room temperature, then the solution was refluxed for 8 h. Upon cooling to room temperature, the solvent was evaporated under *vacuum* and the residue was triturated with ethanol (100 mL). After stirring for 10 min, the precipitant was filtered to give the corresponding crude product. Afterward, the filter cake was transited to anhydrous ethanol (120 mL) and stirred overnight at room temperature. Finally, the suspension liquid was filtered, off dried over $MgSO_4$ to afford **5a-5b.**

*5.1.5.1.2-amino-4-(2,4-difluorophenyl)-6-(1H-indol-3-yl)nicotinonitrile (**5a**)*

Pale yellow solid.Yield: 59.7%. MS (ESI) m/z (%):347.1[M+H]$^+$.

*5.1.5.2. 2-amino-4-(2-chloro-4-fluorophenyl)-6-(1H-indol-3-yl)nicotinonitrile (**5b**)*

Pale yellow solid.Yield: 74.6%. MS (ESI) m/z (%):363.0 [M+H]$^+$.

*5.1.6. General procedure for preparation of 2-(chloromethyl)-5-(1H-indol-3-yl)-7-arylimidazo [1,2-a]pyridine-8-carbonitrile (**6a-6b**)*

To a stirred solution of **5a-5b** (14.4 mmol) in ethanol (50 mL) was added 1,3-dichloropropan-2-one (18.2 g,144.1 mmol). Then the reaction mixture was refluxed and stirred for 10 h. After the completion of the reaction, the solvent was concentrated in *vacuum* and the residue was dissolved in diethyl ether (50 mL) and stirred for 2 h. The corresponding crude products **6a-6b** were obtained by filtration without further purification.

*5.1.6.1. 2-(chloromethyl)-7-(2,4-difluorophenyl)-5-(1H-indol-3-yl)imidazo[1,2-a]pyridine-8-carb onitrile (**6a**)*

Yellow solid.Yield:77.4%. MS (ESI) m/z (%):419.1 [M+H]$^+$.

*5.1.6.2. 7-(2-chloro-4-fluorophenyl)-2-(chloromethyl)-5-(1H-indol-3-yl)imidazo[1,2-a]pyridine-8 -carbonitrile (**6b**)*

Yellow solid. Yield:72.9%. MS (ESI) m/z (%):435.0 [M+H]$^+$.

*5.1.7. General procedure for preparation compounds (**7a-7n**)*

A stirring mixture of an appropriate **6a-6b** (1.2 mmol) and an appropriate*N*-aliphatic amines (1.8 mmol) in ethanol(25 mL) was stirred at reflux for 5 h.After cooling to room temperature, the solvent was evaporated in *vacuum* to afford yellow residue. The formed precipitate was dissolved in DMF and purified on a silica gel column using petroleum ether/ ethyl acetate (3:1) to give pure target product **7a**-**7n**.

*5.1.7.1. 7-(2,4-difluorophenyl)-2-((dimethylamino)methyl)-5-(1H-indol-3-yl)imidazo[1,2-a]pyridi ne-8-carbonitrile (**7a**)*

Pale while solid. Yield: 66.6%.m.p.: 246.9-248.4 ºC. MS(ESI) m/z(%): 428.2 [M+H]$^+$. ^{1}H NMR (400 MHz, DMSO-d_6) δ: 12.17 (s, 1H), 8.25 (d,*J*= 2.0 Hz, 1H), 8.00 (s, 1H), 7.84 (dd,*J*= 15.2, 8.6 Hz, 1H), 7.60 (d,*J* = 8.4 Hz, 2H), 7.57 – 7.51 (m, 1H), 7.34 (td,*J*= 8.5, 2.3 Hz, 1H), 7.28 (t, *J* = 7.7 Hz, 1H), 7.21 – 7.16 (m, 2H), 3.64 (s, 2H), 2.23 (s, 6H).Anal.calcd. for$C_{25}H_{19}F_2N_5$ (%):C, 70.25, H, 4.48, N, 16.38. Found (%):C, 70.19, H, 4.39, N, 16.31.

*5.1.7.2. 7-(2,4-difluorophenyl)-5-(1H-indol-3-yl)-2-((methylamino)methyl)imidazo[1,2-a]pyridine -8-carbonitrile (**7b**)*

Pale while solid. Yield:69.8%.m.p.: 219.3-221.2ºC. MS(ESI) m/z(%): 414.1 [M+H]$^+$.^{1}H

NMR (400 MHz, DMSO-d_6) δ:12.29 (s, 1H), 8.24 (d, J = 2.0 Hz, 1H), 8.19 (s, 1H), 7.83 (dd, J = 15.2, 8.2 Hz, 1H), 7.60 – 7.53 (m, 3H), 7.33 (td, J = 8.5, 2.3 Hz, 1H), 7.27 (t, J = 7.6 Hz, 1H), 7.21 – 7.15 (m, 2H), 4.01 (s, 2H), 2.42 (s, 3H), 1.21 (s, 1H).Anal. calcd. for$C_{24}H_{17}F_2N_5$ (%):C, 69.72, H, 4.14, N, 16.94. Found (%):C, 69.65, H, 4.08, N, 16.89.

*5.1.7.3. 7-(2,4-difluorophenyl)-2-((ethylamino)methyl)-5-(1H-indol-3-yl)imidazo[1,2-a]pyridine-8-carbonitrile (**7c**)*

Pale while solid. Yield: 79.3%. m.p.: 171.1-177.1 ºC.MS(ESI) m/z(%): 428.2 $[M+H]^+$. ^{1}H NMR (400 MHz, DMSO-d_6) δ: 12.32 (s, 1H), 8.26 (s, 1H), 8.13 (s, 1H), 7.83 (dd, J= 15.2, 8.6 Hz, 1H), 7.65 – 7.59 (m, 2H), 7.58 – 7.51 (m, 1H), 7.33 (td,J= 8.5, 2.2 Hz, 1H), 7.27 (t, J = 7.6 Hz, 1H), 7.21 – 7.16 (m, 2H), 3.96 (s, 2H), 2.67 (q, J = 7.1 Hz, 2H), 1.21 (s, 1H), 1.06 (t, J = 7.1 Hz, 3H).Anal.calcd. for$C_{25}H_{19}F_2N_5$ (%):C, 70.25, H, 4.48, N, 16.38. Found (%):C, 70.19, H, 4.42, N, 16.33.

*5.1.7.4. 7-(2,4-difluorophenyl)-5-(1H-indol-3-yl)-2-((isopropylamino)methyl)imidazo[1,2-a]pyridine-8-carbonitrile (**7d**)*

Pale while solid. Yield:79.8%.m.p.: 246.3-248.9 ºC. MS(ESI) m/z(%): 440.1 $[M-H]^+$.^{1}H NMR (400 MHz, DMSO-d_6) δ: 12.25 (d, J = 0.7 Hz, 1H), 8.26 (s, 1H), 8.20 (s, 1H), 7.85 (td, J = 8.6, 6.6 Hz, 1H), 7.62 (t, J = 8.1 Hz, 2H), 7.55 (dd, J = 10.4, 2.4 Hz, 1H), 7.35 (td, J = 8.4, 2.4 Hz, 1H), 7.32 – 7.27 (m, 1H), 7.20 (dd, J = 13.6, 5.7 Hz, 2H), 4.04 (s, 2H), 1.23 (s, 2H), 1.19 (d, J = 6.3 Hz, 1H), 1.10 (d, J = 6.3 Hz, 5H).^{13}C NMR (101 MHz, DMSO) δ:160.97, 158.46, 148.90, 143.76, 137.97, 137.91, 137.00, 133.45, 133.35, 128.86, 125.11, 123.19, 121.37, 119.91, 115.95, 113.21, 112.89, 112.73, 111.30, 107.60, 105.28, 96.32, 48.09, 45.14, 23.02. Anal.calcd. for$C_{26}H_{21}F_2N_5$ (%):C, 70.74, H, 4.79, N, 15.86. Found (%):C, 70.69, H, 4.75, N, 15.80.

*5.1.7.5. 2-((cyclohexylamino)methyl)-7-(2,4-difluorophenyl)-5-(1H-indol-3-yl)imidazo[1,2-a]pyridine-8-carbonitrile (**7e**)*

Pale while solid. Yield:78.4%.m.p.: 193.0-194.8 ºC. MS(ESI) m/z(%): 482.2 $[M+H]^+$.^{1}H NMR (400 MHz, DMSO-d_6) δ: 12.29 (s, 1H), 8.25 (s, 1H), 8.13 (s, 1H), 7.82 (td, J = 8.7, 6.6 Hz, 1H), 7.60 (d, J = 8.6 Hz, 2H), 7.54 (td, J = 10.6, 2.5 Hz, 1H), 7.33 (td, J = 8.4, 2.3 Hz, 1H), 7.30 – 7.24 (m, 1H), 7.22 – 7.09 (m, 2H), 3.99 (s, 2H), 2.00 – 1.78 (m, 2H), 1.66 (d, J = 12.5 Hz, 2H), 1.53 (d, J = 11.7 Hz, 1H), 1.29 – 1.01 (m, 6H). Anal.calcd. for $C_{29}H_{25}F_2N_5$ (%):C, 72.33, H, 5.23, N, 14.54. Found (%):C, 72.27, H, 5.19, N, 14.45.

*5.1.7.6. 7-(2,4-difluorophenyl)-5-(1H-indol-3-yl)-2-(pyrrolidin-1-ylmethyl)imidazo[1,2-a]pyridine-8-carbonitrile (**7f**)*

Pale while solid. Yield:90.6%.m.p.: 200.5-203.2 ºC. MS(ESI) m/z(%): 454.2 $[M+H]^+$.^{1}H NMR (400 MHz, DMSO-d_6) δ: 12.19 (s, 1H), 8.25 (s, 1H), 8.03 (s, 1H), 7.82 (dd, J = 15.2, 8.6 Hz, 1H), 7.60 (s, 1H), 7.58 (s, 1H), 7.57 – 7.50 (m, 1H), 7.33 (td, J = 8.5, 2.2 Hz, 1H), 7.26 (t, J = 7.7 Hz, 1H), 7.20 – 7.14 (m, 2H), 3.86 (s, 2H), 2.61 (s, 4H), 1.69 (s, 4H).Anal.calcd. for$C_{27}H_{21}F_2N_5$ (%):C, 71.51, H, 4.67, N, 15.44. Found (%): C, 71.44, H, 4.58, N, 15.39.

*5.1.7.7. 7-(2,4-difluorophenyl)-5-(1H-indol-3-yl)-2-((4-methylpiperazin-1-yl)methyl)imidazo[1,2-a]pyridine-8-carbonitrile (**7g**)*

Pale while solid. Yield:91.6%.m.p.: 245.1-247.9 ºC. MS(ESI) m/z(%): 482.2 $[M+H]^+$.^{1}H NMR (400 MHz, DMSO-d_6) δ: 12.21 (s, 1H), 8.25 (d, J = 2.3 Hz, 1H), 8.00 (s, 1H),

7.83 (td, *J* = 8.7, 6.6 Hz, 1H), 7.62 – 7.57 (m, 2H), 7.54 (dd, *J* = 10.0, 1.7 Hz, 1H), 7.34 (td, *J* = 8.5, 2.4 Hz, 1H), 7.28 (t, *J* = 7.7 Hz, 1H), 7.21–7.15 (m, 2H), 3.67 (s, 2 H), 2.54–2.45 (m, 8H), 2.14 (s, 3H).^{13}C NMR (101 MHz, DMSO) *δ*:160.81, 158.45, 146.17, 143.77, 138.03, 137.03, 133.44, 133.31, 128.97, 125.03, 123.13, 121.27, 119.91, 115.93, 113.27, 112.94, 112.67, 112.57, 112.39, 107.52, 105.27, 96.43, 56.12, 55.03, 52.92, 45.98.Anal.calcd. f or $C_{28}H_{24}F_2N_6$ (%):C, 69.70, H, 5.01, N, 17.42. Found (%): C, 69.65, H, 4.96, N, 17.35.

*5.1.7.8. 7-(2,4-difluorophenyl)-5-(1H-indol-3-yl)-2-((4-methylpiperidin-1-yl)methyl)imidazo[1,2-a]pyridine-8-carbonitrile (**7h**)*

Pale while solid. Yield:87.4%.m.p.: 219.3-221.0ºC. MS(ESI) m/z(%): 482.1 $[M+H]^+$.^{1}H NMR (400 MHz, DMSO-*d*$_6$) *δ:* 12.16 (s, 1H), 8.23 (s, 1H), 7.97 (s, 1H), 7.81 (td, *J* = 8.6, 6.6 Hz, 1H), 7.57 (t, *J* = 7.3 Hz, 2H), 7.52 (dd, *J* = 9.9, 1.8 Hz, 1H), 7.32 (td, *J* = 8.4, 2.2 Hz, 1H), 7.26 (t, *J* = 7.5 Hz, 1H), 7.18 – 7.13 (m, 2H), 3.65 (s, 2H), 2.88 (d, *J* = 11.1 Hz, 2H), 2.00 (t, *J* = 11.0 Hz, 2H), 1.52 (d, *J* = 11.6 Hz, 2H), 1.19 (s, 1H), 1.13 – 1.04 (m, 2H), 0.83 (d, *J* = 6.4 Hz, 3H).Anal.calcd. for$C_{29}H_{25}F_2N_5$ (%):C, 72.33, H, 5.23, N, 14.54. Found (%): C, 72.27, H, 5.18, N, 14.45.

*5.1.7.9. 2-((cyclopropylamino)methyl)-7-(2,4-difluorophenyl)-5-(1H-indol-3-yl)imidazo[1,2-a]pyridine-8-carbonitrile (**7i**)*

Pale while solid. Yield:81.5%.m.p.: 205.0-207.6ºC. MS(ESI) m/z(%): 426.3 $[M+H]^+$.^{1}H NMR (400 MHz, DMSO-*d*$_6$) *δ:* 12.15 (s, 1H), 8.23 (d, *J* = 2.0 Hz, 1H), 7.98 (s, 1H), 7. 82 (dd, *J* = 15.2, 8.6 Hz, 1H), 7.60 – 7.50 (m, 3H), 7.33 (td, *J* = 8.5, 2.3 Hz, 1H), 7.2 6 (t, *J* = 7.7 Hz, 1H), 7.20 – 7.14 (m, 2H), 3.62 (s, 2H), 2.09 (m, 1H), 1.17 (s, 1H), 0. 79 (m, 4H). Anal.calcd. for$C_{26}H_{19}F_2N_5$ (%):C, 71.06, H, 4.36, N, 15.94. Found (%): C, 71. 01, H, 4.32, N, 15.88.

*5.1.7.10.2-((diethylamino)methyl)-7-(2,4-difluorophenyl)-5-(1H-indol-3-yl)imidazo[1,2-a]pyridine-8-carbonitrile (**7j**)*

Pale while solid. Yield:89.7%.m.p.: 200.3-202.0ºC. MS(ESI) m/z(%): 456.2 $[M+H]^+$.^{1}H NMR (400 MHz, DMSO-*d6*) *δ*: 12.43 (s, 1H), 8.34 (s, 1H), 8.29 (d, *J* = 1.8 Hz, 1H), 7.83 (td, *J* = 8.6, 6.6 Hz, 1H), 7.62 (dd, *J* = 7.9, 4.8 Hz, 2H), 7.53 (td, *J* = 10.7, 2.5 H z, 1H), 7.33 (td, *J* = 8.4, 2.2 Hz, 1H), 7.26 (dd, *J* = 13.4, 4.9 Hz, 2H), 7.16 (t, *J* = 7.5 Hz, 1H), 4.17 (s, 2H), 2.88 (s, 4H), 1.18 (t, *J* = 6.9 Hz, 5H).Anal.calcd. for $C_{27}H_{23}F_2N_5$ (%):C, 71.19, H, 5.09, N, 15.37. Found (%): C, 71.16, H, 4.98, N, 15.33.

*5.1.7.11. 7-(2-chloro-4-fluorophenyl)-5-(1H-indol-3-yl)-2-(morpholinomethyl)imidazo[1,2-a]pyridine-8-carbonitrile (**7k**)*

Pale while solid. Yield: 91.2%. m.p.: 225.1-227.0ºC.MS(ESI) m/z(%): 486.2 $[M+H]^+$.^{1} H NMR (400 MHz, DMSO-*d*$_6$) *δ:*12.21 (s, 1H), 8.25 (d, *J* = 2.3 Hz, 1H), 8.00 (s, 1H), 7.83 (td, *J* = 8.7, 6.6 Hz, 1H), 7.62 – 7.57 (m, 2H), 7.54 (dd, *J* = 10.0, 1.7 Hz, 1H), 7. 34 (td, *J* = 8.5, 2.4 Hz, 1H), 7.28 (t, *J* = 7.7 Hz, 1H), 7.21 – 7.15 (m, 2H), 3.66 (s, 2 H), 3.54 (s, 6H),1.21 (s, 2H).Anal.calcd. for $C_{27}H_{21}F_2N_5O$ (%):C, 69.07, H, 4.51, N, 14.92. Found (%): C, 69.02, H, 4.46, N, 14.87.

*5.1.7.12. 7-(2-chloro-4-fluorophenyl)-5-(1H-indol-3-yl)-2-((4-methylpiperazin-1-yl)methyl)imidazo[1,2-a]pyridine-8-carbonitrile (**7l**)*

Pale while solid. Yield: 63.5%.m.p.: 185.7-187.9ºC. MS(ESI) m/z(%): 499.2 $[M+H]^+$.^{1} H NMR (400 MHz, DMSO-*d*$_6$) *δ*: 12.17 (s, 1H), 8.26 (d, *J* = 2.4 Hz, 1H), 8.04 (s, 1H), 7.77 (dd, *J* = 8.7, 6.2 Hz, 1H), 7.73 (dd, *J* = 8.9, 2.6 Hz, 1H), 7.59 (d, *J* = 8.3 Hz, 2

H), 7.46 (td, *J* = 8.5, 2.6 Hz, 1H), 7.28 (t, *J* = 7.7 Hz, 1H), 7.18 (t, *J* = 7.5 Hz, 1H), 7.13 (s, 1H), 3.67 (s, 2H), 2.64 – 2.42 (m, 8H), 2.15 (s, 3H).Anal.calcd. for$C_{28}H_{24}ClFN_6$ (%): C, 67.40, H, 4.85, N, 16.84. Found (%):C, 67.36, H, 4.79, N, 16.77.

*5.1.7.13.7-(2-chloro-4-fluorophenyl)-2-((cyclohexylamino)methyl)-5-(1H-indol-3-yl)imidazo[1,2-a] pyridine-8-carbonitrile (**7m**)*

Pale while solid. Yield: 79.3%.m.p.: 189.3-190.8 ºC. MS(ESI) m/z(%):498.0 $[M+H]^+$.[1] H NMR (400 MHz, DMSO-d_6) δ: 12.21 (s, 1H), 8.24 (d, *J* = 2.4 Hz, 1H), 8.18 (s, 1H), 7.78 – 7.70 (m, 2H), 7.59 (d, *J* = 8.3 Hz, 2H), 7.45 (td, *J* = 8.5, 2.6 Hz, 1H), 7.27 (t, *J* = 7.5 Hz, 1H), 7.20 – 7.13 (m, 2H), 3.99 (s, 2H), 2.43 (m, 1H), 1.79 (m, 5H), 1.36 (m, 5H), 1.17 (s, 1H).Anal.calcd. for $C_{29}H_{25}ClFN_5$ (%):C, 69.94, H, 5.06, N, 14.06. Found (%): C, 69.88, H, 5.00, N, 13.97.

*5.1.7.14. 7-(2-chloro-4-fluorophenyl)-5-(1H-indol-3-yl)-2-((methylamino)methyl)imidazo[1,2-a]p yridine-8-carbonitrile (**7n**)*

Pale while solid. Yield: 83.3%.m.p.: 219.5-223.5 ºC. MS(ESI) m/z(%): 430.1 $[M+H]^+$.[1] H NMR (400 MHz, DMSO-d_6) δ: 12.23 (s, 1H), 8.26 (s, 1H), 8.20 (s, 1H), 7.78 (dd, *J* = 8.6, 6.3 Hz, 1H), 7.75 – 7.71 (m, 1H), 7.65 – 7.57 (m, 2H), 7.47 (td, *J* = 8.5, 2.6 Hz, 1H), 7.29 (t, *J* = 7.5 Hz, 1H), 7.20 (d, *J* = 7.6 Hz, 1H), 7.17 (d, *J* = 4.1 Hz, 1H), 4.01 (s, 2H), 2.43 (s, 3H).Anal.calcd. for$C_{24}H_{17}ClFN_5$ (%):C, 67.06, H, 3.99, N, 16.29. Found (%): C, 66.97, H, 3.93, N, 16.25.

5.2. Biological evaluation

5.2.1. MTT assay

The cytotoxic activity of compounds (**3a**-3**q** and**7a**-7**n**) was evaluated against HT-29,H460, A549, MKN-45 and SMMC-7721 cells by the MTT assay *in vitro*, with Colchicine and CA-4 as references. The cancer cells were cultured in minimum essential medium (MEM) supplemented with 10% fetal bovine serum (FBS). Approximately 4×10^3 cells, suspended in MEM medium, were plated onto each well of a 96-well plate and incubated in 5% CO_2 at 37°C for24 h. The tested compounds were added to the culture medium at the indicated final concentrations and the cell cultures were continued for 72 h. Fresh MTT was added to each well at a final concentration of 5.0μg/mL and incubated with cells at 37 °C for 4 h. The formazan crystals were dissolved in 100.0 μL DMSO per each well, and the absorbency at 492 nm (for the absorbance of MTT formazan) and 630 nm (for the reference wavelength) was measured with the ELISA reader. All of the compounds were tested three times in each of the cell lines. The results expressed as IC_{50} (inhibitory concentration of 50%) were the mean ± SD and were calculated by using the Bacus Laboratories Incorporated Slide Scanner (Bliss) software.

5.2.2. Immunofluorescence staining

Immunostaining was carried out to detect tubulin protein after exposure to CA-4 and **7e**. The HT-29 cell was seeded at 1×10^4 per well on a 24 well plate and grown for 24 h. Cells were treated with CA-4 or **7e** for 24 h. Cells in the control group were treated with culture medium. The control and treated cells were fixed with 4% formaldehyde in PBS for 30 min at -20ºC, then washed three times with PBS and permeabilized with 0.2% (v/v) Triton X-100 in PBS for 20 min. Then, the cells were blocked with 5% bovine serum albumin (BSA) in PBS for 30 min. The primary a-tubulin antibody was diluted (1:100) with 2% BSA in PBS and incubated overnight at 4 ºC. The

cells were washed with PBS to remove unbound primary antibody and then cells were incubated with FITC-conjugated antimousesecondary antibody, diluted (1:100) with 2% BSA in PBS, for 2 h at 37 ºC. The cells were washed with PBS to remove unboundsecondary antibody, nucleus was stained with 4,6-diamino-2-phenolindoldihydrochloride (DAPI) and then, immunofluorescence was detected using a fluorescence microscope (Olympus, Tokyo, Japan).

5.2.3. Competitive tubulin-binding assay

Tubulin was coin cubated with various concentrations of Taxol, **7e** or CA-4 respectively at 37ºC for 1 h. Then colchicine was added to a final concentration of 5 μM. Fluorescence was determined using a Hitachi F-2500 spectrofluorometer (Tokyo, Japan) at excitation wavelengths of 365 nm and emission wavelengths of 435 nm. Blank values (buffer alone) as background were subtracted from all samples. Then the inhibition rate (IR) was calculated as follows: IR=(F÷F0)×100 % where F0 is the fluorescence of the 5 μM colchicine-tubulin complex, and F is the fluorescence of a given concentration of Taxol, **7e** or CA-4 (0 μM, 1.6 μM, 5 μM and 15 μM) competition with the 5 μM colchicine-tubulin complex. Taxol, not binding in the colchicine-site of tubulin, was added as a negative control.

5.2.4. Molecular Docking

The molecular modeling studies were performed with Accelrys Discovery Studio 3.5. The crystal structure of tubulin complexed with DAMA-colchicine (PDB code: 4O2B) was retrieved from the RCSB Protein Data Bank (http://www.rcsb.org/pdb/). In the docking process, the protein protocol was prepared by several operations, including standardization of atom names and insertion of missing atoms in residues. Then, the receptor model was typed with the CHARMm force field and a binding sphere with radius of 15.0 Å was defined through the original ligand (DAMA-colchicine) as the binding site. The Crolibulin and **7e** were drawn with Chemdraw and fully minimized using the CHARMm force field. Finally, they were docked into the binding site using the CDOCKER protocol with the default settings.

Acknowledgments

The work was supported by National Natural Science Foundation of China (No. 81273357), Doctoral Research Foundation of Shenyang Medical College (No. 2014-3057) and Development Project of Ministry of Education Innovation Team (No. IRT1073).

References

[1] K.H. Downing, Structural basis for the interaction of tubulin with proteins and drugs that affect microtubule dynamics, Annu. Rev. Cell Dev. Biol. 16 (2000) 89-111.

[2] L.A. Amos, Microtubule structure and its stabilization, Org. Biomol. Chem.2 (2004) 2153-2160.

[3] A.L.Risinger, F.J. Giles, S.L. Mooberry, Microtubule dynamics as a target in oncology, Cancer Treat. Rev.35 (2009) 255-261.

[4] C. Dumontet, M. A. Jordan, Microtubule-binding agents: a dynamic field of cancer therapeutics, Nat. Rev. Drug Discovery. 9 (2010) 790-803.

[5] C. Kanthou, G. M. Tozer. Microtubule depolymerizing vascular disrupting agents: novel therapeutic agents for oncology and other pathologies. Int.J.Exp.Pathol. 90(2009) 284-294.

[6] Y. Lu, J. Chen, M. Xiao, W. Li, D.D. Miller, An overview of tubulin inhibitors that interact with the colchicine

binding site, Pharm. Res. 29 (2012) 2943-2971.

[7] A.Brossi, H. J.Yeh, M.Chrzanowska, J. Wolff, E. Hamel, C. M. Lin, F. Quin, M.Suffness, J. Silverton,Colchicine and its analogues: recent findings, Med. Res. Rev. 8 (1988)77-94.

[8] B.I. Roman, T.S.Heugebaert, M.E. Bracke, C.V. Stevens. Assessment of the antineoplastic potential of chalcones in animal models. Curr. Med. Chem. 20(2013) 186-221.

[9] G. Markel, M. Imazio, A. Brucato, Y. Adler. Prevention of Recurrent Pericarditis With Colchicine in 2012. Clin. Cardiol. 36(2013) 125-128.

[10]C. M. Lin, H. H.Ho, G. R. Pettit, E.Hamel,Antimitotic natural products combretastatin A-4 and combretastatin A-2: studies on the mechanism of their inhibition of the binding of colchicine to tubulin, Biochemistry. 28 (1989) 6984-6991.

[11] W. Kemnitzer,J.Drewe,S. Jiang,H. Zhang,Y. Wang,J. H. Zhao,C. C. Grundy, L. F. Xu,S. Lamothe,H.Gourdeau, R. Denis, B. Tseng, S.Kasibhatla, S. X.Cai, Discovery of 4-aryl-4H-chromenes as a new series of apoptosis inducers using a cell- and caspase-based high-throughput screening assay. 3. Structure-activity relationships of fused rings at the 7,8-positions,J. Med. Chem. 50 (2007)2858-2864.

[12] K.Bonezzi, G. Taraboletti, P. Borsotti, F. Bellina, R. Rossi, R. Giavazzi. Vascular Disrupting Activity of Tubulin-Binding 1,5-Diaryl-1H-imidazoles. J. Med. Chem. 52 (2009) 7906-7910.

[13] J. Kaffy, R. Pontikis, D. Carrez, A. Croisy, C. Monneret, J.C. Florent.Isoxazole-type derivatives related to combretastatin A-4, synthesis and biological evaluation. Bioorg. Med. Chem. 14 (2006) 4067-4077.

[14]S.Theeramunkong, A. Caldarelli, A. Massarotti, S. Aprile, D. Caprioglio, R. Zaninett, A. Teruggi, T. Pirali, G. Grosa, G.C. Tron, A.A. Genazzani. Regioselective Suzuki Coupling of Dihaloheteroaromatic Compounds as a Rapid Strategy to Synthesize Potent Rigid Combretastatin Analogues. J. Med. Chem.54 (2011) 4977-4986.

[15] E. Hamel. Antimitotic natural products and their interactions with tubulin. Med. Res. Rev. 16 (1996) 207-231.

[16] R. Shirai, H. Takayama, A. Nishikawa, Y. Koiso, Y. Hashimoto. Asymmetric synthesis of antimitotic combretadioxolane with potent antitumor activity against multi-drug resistant cells. Bioorg. Med. Chem. Lett. 8(1998) 1997-2000.

[17] H.P. Hsieh, J.P. Liou, N. Mahindroo. Pharmaceutical Design of Antimitotic Agents Based on Combretastatins. Curr. Pharm. Design. 11(2005) 1655-1677.

[18] T.M. Beale, P.J. Bond, J.D. Brenton, D.S. Charnock-Jones, S.V. Ley, R.M. Myers. Increased endothelial cell selectivity of triazole-bridged dihalogenated A-ring analogues of combretastatin A-1. Bioorg. Med. Chem. 20 (2012) 1749 – 1759.

[19] J.Kalmuk, M.Folaron, J.Buchinger, R. Pili, M.Seshadri, Multimodal imaging guided preclinical trials of vascular targeting in prostate cancer, Oncotarget.6 (2015) 24376-24392.

[20] S. X. Cai, J. Drewe, W. Kemnitzer, Discovery of 4-aryl-4H-chromenes as potent apoptosis inducers using a cell- and caspase-based Anti-cancer Screening Apoptosis Program (ASAP): SAR studies and the identification of novel vascular disrupting agents, Anticancer Agents Med. Chem. 9 (2009) 437-456.

[21] W. Kemnitzer, J.Drewe, S. Jiang, H. Zhang, Y. Wang, J. Zhao, S.Jia,J.Herich, D.Labreque, R.Storer, K.Meerovitch, D.Bouffard, R.Rej,R. Denis, C.Blais, S.Lamothe,G.Attardo, H.Gourdeau, B. Tseng,S.Kasibhatla,S. X.Cai. Discovery of 4-aryl-4H-chromenes as a new series of apoptosis inducers using a cell- and caspase-based high-throughput screening assay. 1. Structure-activity relationships of the 4-aryl group, J. Med. Chem.47 (2004) 6299-6310.

[22] T.Meng, W.Wang, Z.X.Zhang, L.P. Ma, Y.L.Zhang, Z. H. Miao, J.K. Shen,Synthesis and biological evaluation of 6H-pyrido[2',1':2,3]imidazo[4,5-c]isoquinolin-5(6H)-ones as antimitotic agents and inhibitors of tubulin polymerization, Bioorg. Med. Chem. 22 (2014) 848-855.

[233] M.E.Welsch, S.A.Snyder, B.R.Stockwell. Privileged scaffolds for library design and drug discovery. Curr.

Opin. Chem. Biol.14 (2010) 347-361.

[24] Qian, X., A. McDonald, H.J. Zhou, et al. Discovery of the First Potent and Selective Inhibitor of Centromere-Associated Protein E: GSK923295. ACS.Med.Chem. Lett. 1(2010) 30-34.

[25] T. Hirayama, M. Okaniwa , H. Banno, H. Kakei, A. Ohashi, K. Iwai, M. Ohori, K. Mori, M. Gotou, T. Kawamoto, A. Yokota, T. Ishikawa. Synthetic Studies on Centromere-Associated Protein-E (CENP-E) Inhibitors: 2. Application of Electrostatic Potential Map (EPM) and Structure-Based Modeling to Imidazo[1,2-a]pyridine Derivatives as Anti-Tumor Agents. J. Med. Chem. 8(2015)8036-8053.

[26] M. Mantri, O. Graaf, J. vanVeldhoven,A.Göblyös,J. K. von FrijtagDrabbeKünzel, T. Mulder-Krieger, R. Link, H. de Vries, M. W.Beukers, J.Brussee, A. P.Ijzerman, 2-Amino-6-furan-2-yl-4-substituted nicotinonitriles as A2A adenosine receptor antagonists, J. Med. Chem. 51 (2008) 4449-4455.

[27] H. M. Liao, L. E. Chong, L. Tan, X. D. Chen, R. You, P. Gong,Synthesis and biological evaluation of novel 5, 7-diphenylimidazo[1,2-a]pyridine derivatives, Chem. Res. Chin. Univ. 30 (2014) 759-763.

[28] O. Ottoni, A. Neder, A. K. Dias, R. P. Cruz, L. B. Aquino,Acylation of indole under Friedel-Crafts conditions-an improved method to obtain 3-acylindoles regioselectively,Org. Lett. 3 (2001) 1005-1007.

[29] M.V. Reddy, B. Akula, S.C. Cosenza, C.M. Lee, M.R. Mallireddiqari, V.R. Pallela, D.R. Subbaiah, A. Udafa, E.P. Reddy. (*Z*)-1-Aryl-3-arylamino-2-propen-1-ones, Highly Active Stimulators of Tubulin Polymerization: Synthesis, Structure–Activity Relationship (SAR), Tubulin Polymerization, and Cell Growth Inhibition Studies. J. Med. Chem. 55(2012) 5174-5187.

[30]A. Rai, A. Surolia, D. Panda. An antitubulin agent BCFMT inhibits proliferation of cancer cells and induces cell death by inhibiting microtubule dynamics. *Plos One.* 7(2012)e44311.

[31] B. Bhattacharyya, J. Wolff. Promotion of fluorescence upon binding of colchicine to tubulin. Proc. Nat. Acad. Sci. USA. 71(1974)2627-2631.

[32] Y. Lu, J. Chen, M. Xiao, W. Li, D.D. Miller. An overview of tubulin inhibitors that interact with the colchicine binding site. Pharma. Res. 29(2012) 2943-2971.

Graphical Abstract

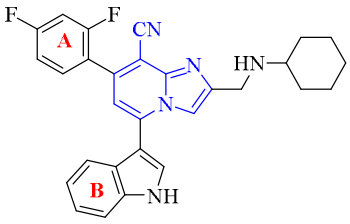

7e

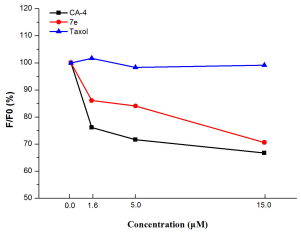

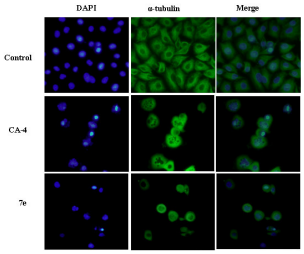

- Two series of novel IMP derivatives (**3a-3q** & **7a-7n**) were designed and synthesized.
- **7e** showed better cytotoxicity against tested cells than CA-4 and Crolibulin.
- Immunofluorescence assay ascertain the mitotic machinery interfering potency of **7e**.
- Colchicine competitive binding assay showed that **7e** binds at colchicine site.
- Docking mode revealed **7e** could overlap well with Crolibulinin the colchcine site.